

Fig. S1: Liver phenotypes of *Depdc5^{Δhep}* mice. **a**, Liver sections were subjected to H&E staining and anti-phospho-S6 immunostaining for 2-month-old females of the Fig. 1 cohort. Boxed areas are magnified in the insets. **b, c**, After 12 hours of fasting, 2-month-old *Depdc5^{F/F}* and *Depdc5^{Δhep}* littermate mice of indicated gender were injected with 400 mg/Kg of APAP. After 8 hours, livers were collected and analyzed by H&E staining (**b**) and immunoblotting (**c**). Damaged areas (n≥8) and band intensities (n=3) were quantified. **d, e**, Liver lysates from 5-month-old *Depdc5^{F/F}* and *Depdc5^{Δhep}* littermate male mice were subjected to immunoblotting (upper panels) and quantification (lower panels; n=4) to analyze mTORC1 signaling (**d**) and fibrogenic markers (**e**). **f, g**, Two-month-old *Depdc5^{F/F}* and *Depdc5^{Δhep}* littermate male mice were kept on normal chow (LFD) (**f**) or high fat diet (HFD) (**g**) for three additional months. Livers from the 5-month-old mice were subjected to Oil Red O (ORO) staining. ORO-positive areas were quantified (right panels, n=3). Boxed areas are magnified in right panels. **h**, Body weight was monitored during HFD feeding (male, n=8; female, n≥4). Data are presented as mean ± SEM. *P < 0.05; ***P < 0.001; ****P < 0.0001 (Student's t-test). When multiple parameters were assessed, the Holm-Šídák method was used to compare groups (\$, P<0.05; \$\$, P<0.01; \$\$\$\$, P<0.0001). Scale bars, 200 μm.

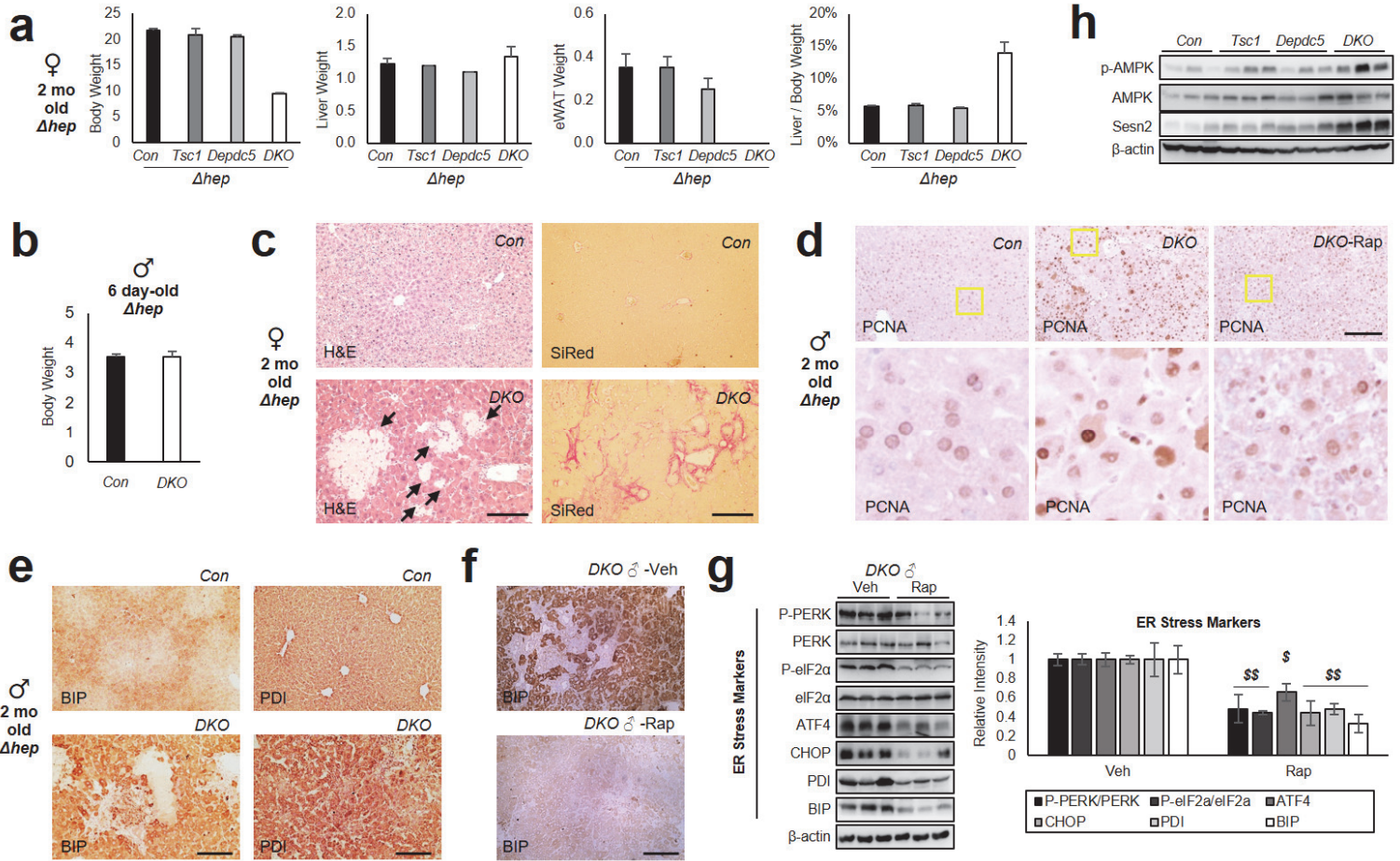


Fig. S2: DKO mice exhibit mTORC1-dependent liver pathologies. **a**, Body, liver, eWAT weights, and liver/body weight ratios were analyzed for females of the Fig. 2 cohort ($n \geq 3$ for Con and DKO; $n=2$ for single knockouts). **b**, Body weights were analyzed for male pups at 6 days after birth ($n \geq 3$). **c**, H&E and SiRed staining images from livers of the Fig. 2 female cohort. **d**, **e**, PCNA (**d**), BIP and PDI (**e**) immunostaining images from livers of the Fig. 2 male cohort. Boxed areas are magnified in bottom panels (**d**). **f**, BIP immunostaining images from livers of the Fig. 4 cohort. **g**, Immunoblotting of ER stress markers (left panel) and quantification (right panel, $n=3$) for livers of the Fig. 4 cohort. β -actin image is the same as the one presented in Fig. 4f. **h**, Immunoblotting of indicated proteins for livers of the Fig. 3 cohort. Data are presented as mean \pm SEM. The Holm-Šídák method was used for multiple comparison tests (\$, $P < 0.05$; \$\$, $P < 0.01$). Scale bars, 200 μ m.

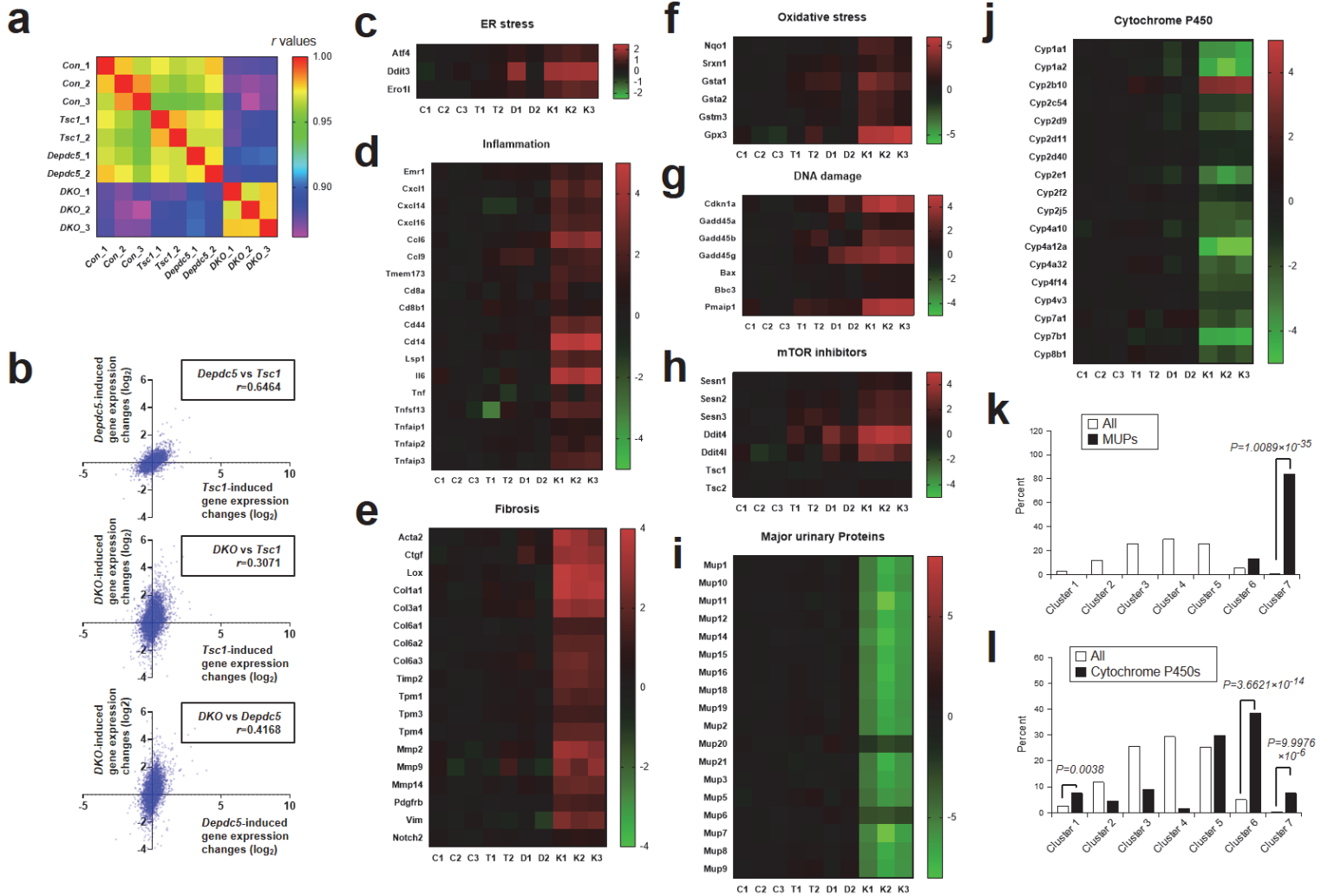


Fig. S3: The DKO transcriptome profile is distinct from controls and single knockout mutants and is characterized by stress response. **a**, Heat map diagram depicting the correlation between individual RNA-seq profiles. **b**, Comparison of mRNA expression fold change over control liver samples between indicated liver samples. Individual dots represent single mRNA species. **c-j**, Heat map diagrams representing mRNA expression fold change from averaged control values (expressed as log₂ values). Each column represents a liver sample from a different *Con* (C1-3), *Tsc1*^{Ahep}(T1-2), *Depdc5*^{Ahep}(D1-2), or *DKO* (K1-3) mouse. **k**, Gene cluster enrichment analysis of major urinary proteins (MUPs). **l**, Gene cluster enrichment analysis of Cytochrome P450s. Correlations between RNA-seq datasets were assessed by computing a nonparametric Spearman correlation (*r*); *P*<0.0001 for all correlation observations. Statistical significance of gene enrichments in a specific cluster was examined by Fisher's exact test.

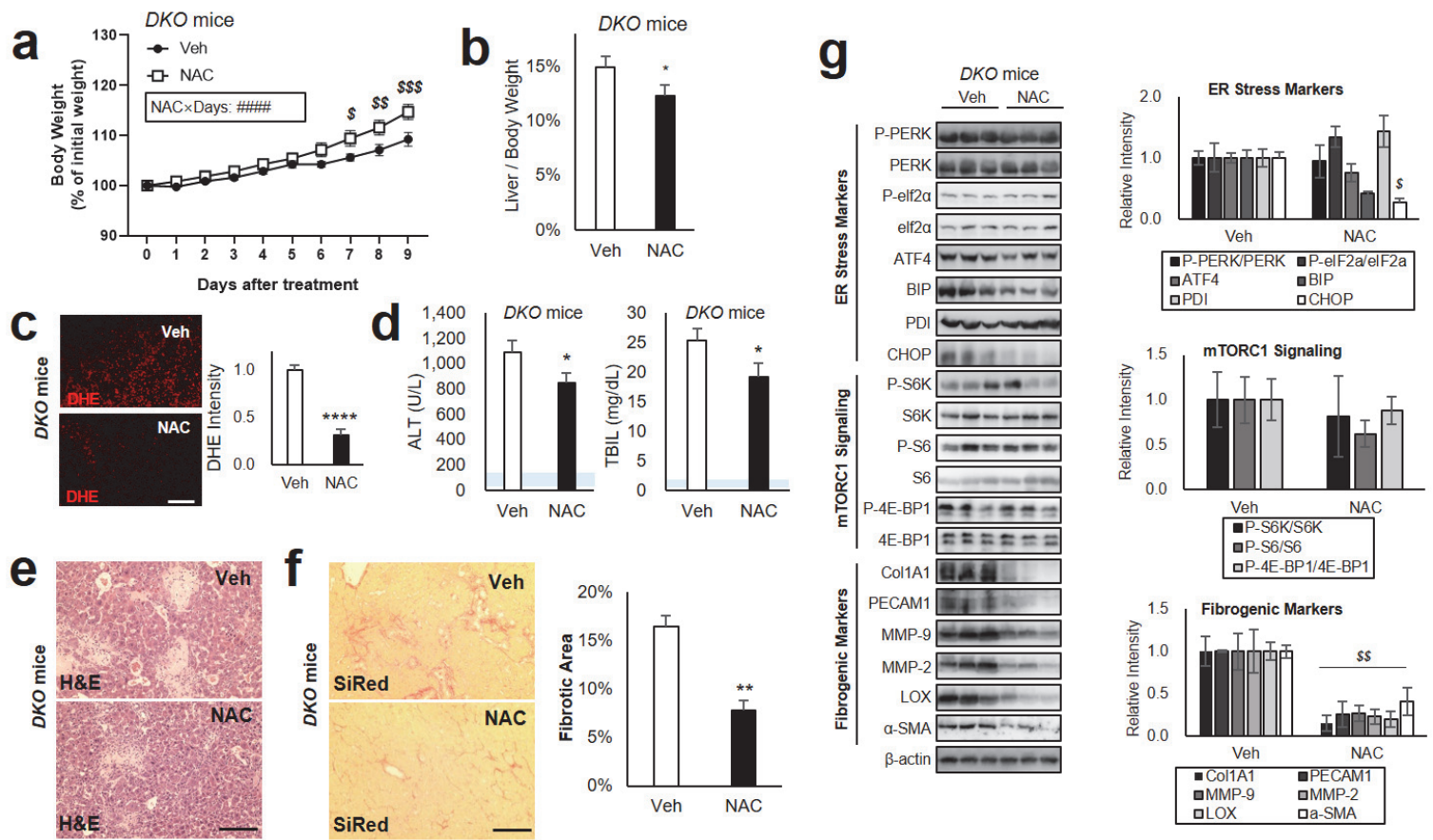


Fig. S4: N-acetylcysteine (NAC) relieves DKO liver pathologies. Littermate cohorts of six-week-old DKO mice were injected daily with vehicle (Veh) or NAC (250 mg/kg) for 10 days ($n \geq 10$). For drug treatment experiments, mice were gender-matched with both males and females. **a**, Body weight was monitored throughout the course of the experiment. **b**, Liver/body weight ratio was measured at the experimental endpoint. **c**, Dihydroethidium (DHE) staining of liver sections and quantification. Blue shaded regions indicate clinically normal ranges. **e**, Liver sections were analyzed by H&E staining. **f**, Liver sections were analyzed by SiRed staining. Fibrotic areas were quantified. **g**, Liver lysates were subjected to immunoblotting (left panels) and quantification (right panels) to examine ER stress markers (top), mTORC1 signaling (middle), and fibrogenic markers (bottom). Data are presented as mean \pm SEM. * $P < 0.05$; ** $P < 0.01$; **** $P < 0.0001$ (Student's t-test). Interaction between NAC and treatment days (NAC \times Days) were assessed through RM two-way ANOVA (####, $P < 0.0001$), and differences in individual data points were assessed through Sidak's multiple comparison test (\$, $P < 0.05$; \$\$, $P < 0.01$; \$\$\$, $P < 0.001$). For western blot quantification, the Holm-Šídák method was used to compare groups (\$, $P < 0.05$; \$\$, $P < 0.01$). Scale bars, 200 μ m.

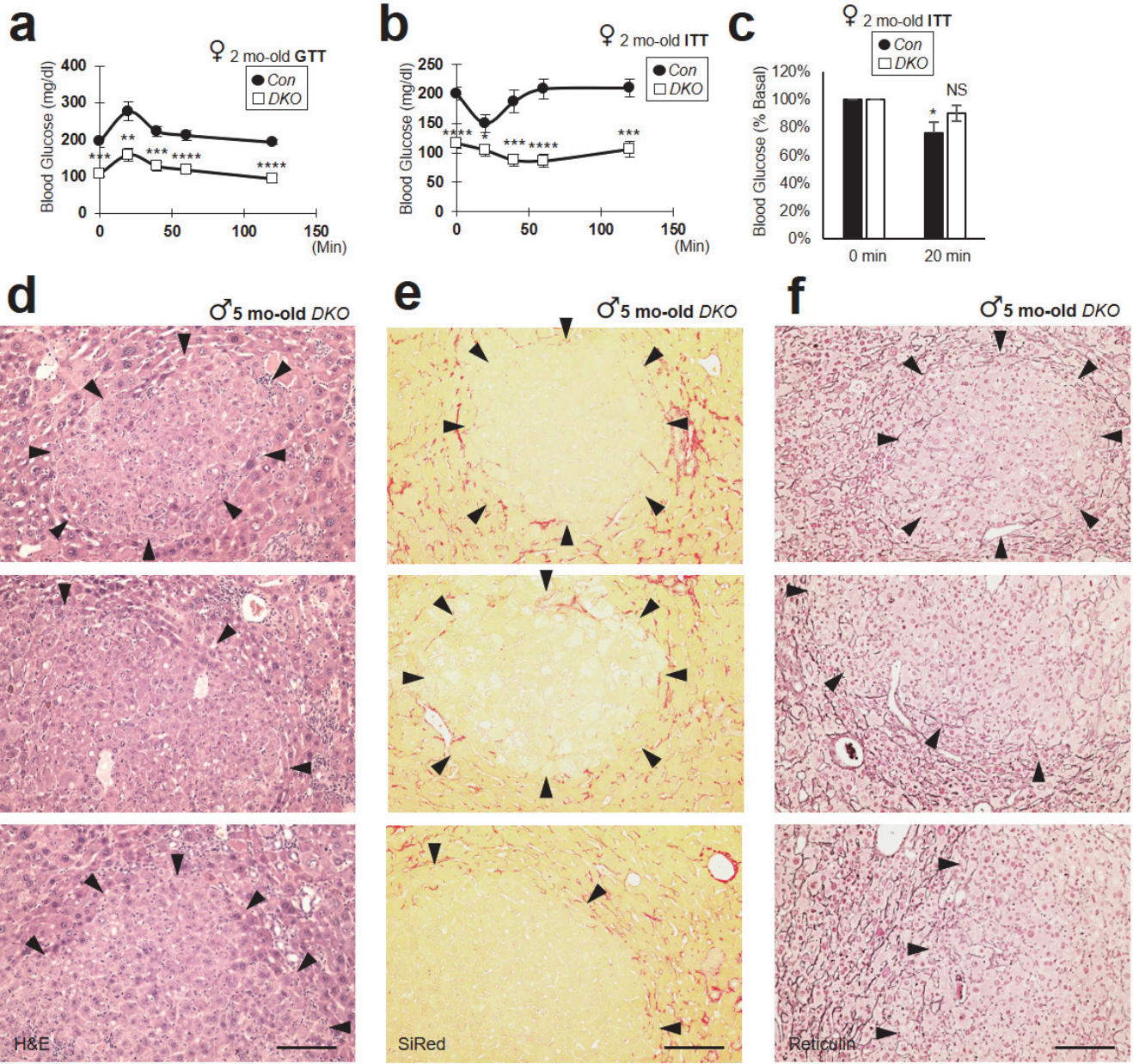


Fig. S5: DKO mice have glucose metabolism defects and HCC development. **a-c**, After 4-6 hours of fasting, two-month-old *Con* and *DKO* female littermates ($n \geq 7$) were subjected to (a) glucose and (b) insulin tolerance tests (GTT and ITT, respectively). Data are normalized according to baseline glucose levels (c). **d-f**, Additional histology images for Fig. 8e upper right (d), 8e middle left (e) and 8e middle right (f) are presented. Arrowheads indicate approximate boundaries of tumor nodules. Data are presented as mean \pm SEM. * $P < 0.05$, ** $P < 0.01$, *** $P < 0.001$, **** $P < 0.0001$, NS ($P = 0.1050$) from a Student's t-test. Scale bars, 200 μ m.